ISSN (Print) 1226-1750
ISSN (Online) 2233-6656
Journal of Magnetics 17(4), 285-290 (2012) http://dx.doi.org/10.4283/JMAG.2012.17.4.285

Comparisons of Linear Characteristic for Shape of Stator Teeth of Hall Effect Torque Sensor

Boram Lee[1], Young Sun Kim[2]*, and Il Han Park[1]

[1]*School of Information and Communication Engineering, Sungkyunkwan University, Suwon 440-746, Korea*
[2]*Department of Electrical and Electronic Engineering, Joongbu University, Geumsan 302-702, Korea*

(Received 25 November 2012, Received in final form 4 December 2012, Accepted 12 December 2012)

Electric Power Steering (EPS) system is superior to conventional Hydraulic Power Steering (HPS) system in aspect of fuel economy and environmental concerns. The EPS system consists of torque sensor, electric motor, ECU (Electric Control Unit), gears and etc. Among the elements, the torque sensor is one of the core technologies of which output signal is used for main input of EPS controller. Usually, the torque sensor has used torsion bar to transform torsion angle into torque and needs linear characteristic in terms of flux variation with respect to rotation angle of permanent magnet. The torsion angle of both ends of a torsion bar is measured by a contact variable resistor. In this paper, the sensor is accurately analyzed using 3D finite element method and its characteristics with respect to four different shapes of the stator teeth are compared. The four shapes are rectangular, triangular, trapezoidal and circular type.

Keywords : Electric Power Steering (EPS), torque sensor, Finite Element Method (FEM), shape design, hall effect

1. Introduction

Nowadays, cars are one of the essential elements in our life. However, they are main culprits for environmental problems and energy waste. Therefore, reducing the environmental impacts of cars is one of the most urgent tasks to be dealt with. With various technologies being developed for the purpose, there are on-going efforts to replace existing auto parts with new ones that are more eco-friendly and energy-efficient. These methods seem to be feasible in the near future. As another method, electricity is utilized to enhance energy efficiency and reduce weight, making cars more environmentally friendly.

Power steering system is set up to improve driver's convenience and steering accuracy. HPS (Hydraulic Power Steering) system, which is a kind of power steering system, uses hydraulic pressure, supplemental power from an engine as shown in Fig. 1. The system rotates wheels in accordance with driver's steering will. It operates a hydraulic pump with the power generated from the engine. This system has some weaknesses, such as too complicated and heavy structure; and, due to the use of engine power, low engine output and fuel efficiency. EPS (Electric Power Steering) system is in the making to solve the problems of HPS system. EPS system is an equipment to supplement driver's steering through an electric motor. It has many benefits. First, car weight will be reduced by the removal of complicated hydraulic equipments. Second, the environmental impact will lessen because it doesn't use oil. Third, fuel efficiency will be enhanced with an electric motor running only when steering happens [1].

EPS system consists of an electric motor, ECU (Electric Control Unit), torque sensor etc. In particular, a torque sensor is one of the core parts in the system. It measures driver's steering will and sends the results to the ECU, which, in turn, commands the electric motor to generate supplemental power. Many countries are studying EPS

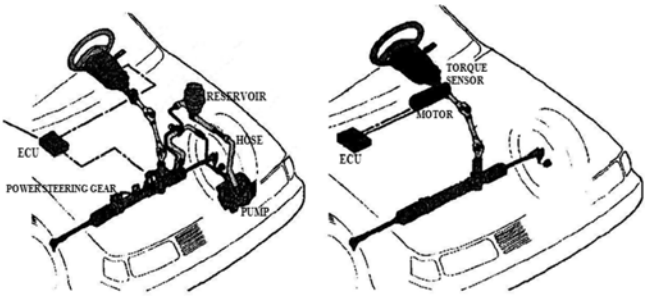

Fig. 1. HPS system and EPS system.

*Corresponding author: Tel: +82-41-750-6279
Fax: +82-41-750-6402, e-mail: yskim@joongbu.ac.kr

systems and some have succeeded in developing the systems.

In this paper, the Hall effect torque sensor is accurately analyzed using 3D FEM. Normally, 2D FEM is used in Finite Element Analysis. In this case, it is necessary to assume that the length of the analyzed model is infinite in a certain direction. However, a torque sensor is small in size and of complex structure, which means that 2D method must be replaced with 3D method. Also, characteristic of flux density measured by Hall sensor should represents linear changes to rotating angle to catch an angle of steering wheel accurately. This characteristic depends on the shape of stator teeth. Finally, various types of stator teeth are proposed to achieve this purpose. The results can provide the various data to machine designers according to the shape of teeth and permanent magnet array.

2. Hall Effect Torque Sensor of EPS System

EPS systems are designed to operate a motor with electric power generated from a battery and create steering torque through a reduction gear on the steering column. A torque sensor measures steering angles and controls a steering column according to the angles, providing stability at high speeds and steering convenience at low speeds.

Fig. 2 illustrates the structure and process of an EPS system [2]. When a driver turns a steering wheel, torque is generated between output and input columns. Such torque is transformed into torsion angles by the torsion bar connecting output and input columns. At this point, the torque sensor detects the torsion angles and changes them into electric signals, which will be sent to the ECU. Then, the ECU adjusts torque according to the signals and operates a motor to offset the torque. As a result, the driver is able to control a steering system with less effort.

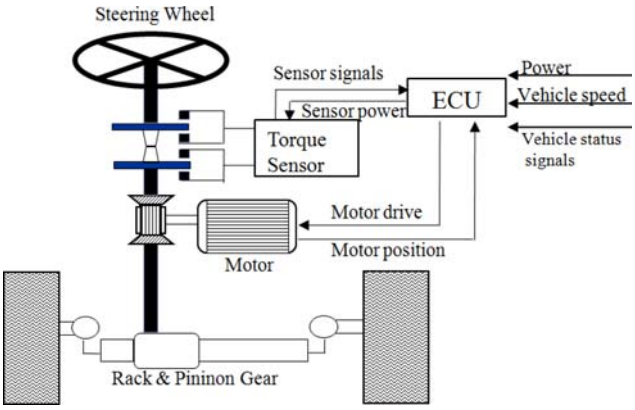

Fig. 2. (Color online) Structure and driving process of EPS system. Here, ECU requires accurate information on the torque applied by driver to the steering wheel. This torque signal usually comes from the shift measurement between two shafts linked by a linear torsion bar.

A torque sensor is one of the core technologies in the EPS system for reducing steering effort. The sensor identifies torque a driver's strength to turn a steering wheel, directions of rotation, and steering angles. After that, it figures out necessary degrees and directions of supplemental power for changing driving conditions. A torque sensor is mainly divided into two functional parts. The one is for measuring torsion angles of the torsion bar, and the other is for effectively transmitting the torsion angles to an ECU.

Largely, there are two types of torque sensor: contact and non-contact. In the beginning, contact types, which measure torsion angles of both ends of a torsion bar using a contact variable resistor, are most used. However, their signal processing is not accurate and the maintenance is difficult. So, now, non-contact types are preferred to contact ones. Noncontact types are, again, divided into some subtypes. Among them, "inductance type" is using coils to measure torque by inductance changes. "Optical type" is using optical devices. "Hall type" is using Hall Effect [3, 4].

Fig. 3 shows a Hall effect torque sensor, the analyzed model in this paper. A Hall effect torque sensor is composed of permanent magnets, stators, collector, and Hall IC. Permanent magnets generate magnetic flux. Stators draw such flux into one spot in a linear manner according to torsion angles. Hall IC identifies the magnetic flux in the collector. The mechanism of the torque sensor is as followed. The permanent magnet located in the base point creates magnet flux, which will pass between upper and lower teeth. In this case, magnetic flux density in the Hall IC is zero. However, if the permanent starts to rotate, the balance between the upper and lower teeth is broken, resulting in movement of magnetic flux to the Hall sensor.

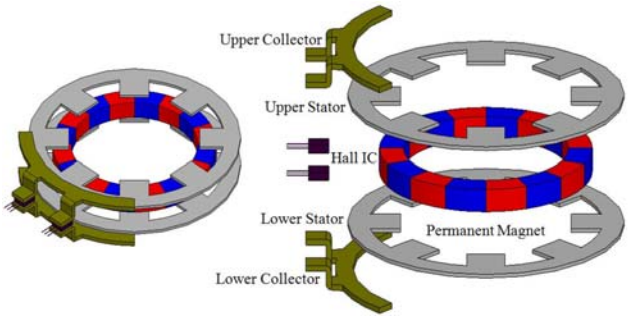

Fig. 3. (Color online) Exploded view of the Hall effect torque sensor. Each segment of permanent magnet generate magnetic flux which are measured by Hall IC according to rotating angle of magnet.

The Hall sensor identifies measures torsion angles. The Hall IC needs a Hall type sensor, which transforms magnetic flux into voltage signals by using Hall effect.

3. Formulation for 3D Finite Element Analysis

Ampere's circuital law, irrespective of the displacement current, is defined as (1) [5]

$$\nabla \times \vec{H} = \vec{J} \tag{1}$$

where $\vec{H}$ is magnetic field intensity [A/m] and $\vec{J}$ is current density [A/m^2]. With a permanent magnet, magnetic flux density $\vec{B}$ [T] can be calculated using (2).

$$\vec{B} = \mu_0(\vec{H} + \vec{M}) \tag{2}$$

where μ_0 is permeability of vacuum [H/m], $\vec{M}$ is magnetization of the permanent magnet [A/m]. When $\vec{M}$ is redivided by magnetization $\vec{M}_0$, which constantly exists in the permanent magnet, (3) will result.

$$\vec{M} = \chi\vec{H} + \vec{M}_0 \tag{3}$$

where χ is magnetic susceptibility. When (3) is applied to (2), the final form of magnetic flux density can be expressed by using the residual magnetic flux density, $\vec{B}_r$, as [6].

$$\vec{B} = \mu_0(\vec{H} + \chi\vec{H} + \vec{M}_0) = \mu_0(1+\chi)\vec{H} + \mu_0\vec{M}_0 = \mu\vec{H} + \vec{B}_r \tag{4}$$

(5) can result from the relation between magnetic flux density and magnetic vector potential.

$$\vec{B} = \nabla \times \vec{A} \tag{5}$$

Where A denotes the magnetic vector potential including x, y and z-components. Accordingly, when (4) and (5) are applied to (1), a governing equation of the magnetic field including the permanent magnet will be produced.

$$\nabla \times \nu(\nabla \times \vec{A} - \vec{B}_r) = \vec{J} \tag{6}$$

Where ν is magnetic resistivity [m/H]. When the above governing equation is formulated by tetrahedron element using 3D Finite element method, equation (7), a 12 by 12 element matrix will result as follow [7-10].

$$\begin{bmatrix} K_{11} & K_{12} & K_{13} & K_{14} \\ K_{21} & K_{22} & K_{23} & K_{24} \\ K_{31} & K_{32} & K_{33} & K_{34} \\ K_{41} & K_{42} & K_{43} & K_{44} \end{bmatrix} \begin{Bmatrix} \vec{A}_1 \\ \vec{A}_2 \\ \vec{A}_3 \\ \vec{A}_4 \end{Bmatrix} = \begin{Bmatrix} \vec{F}_1 \\ \vec{F}_2 \\ \vec{F}_3 \\ \vec{F}_4 \end{Bmatrix} \tag{7}$$

Here, K_{ij} are matrix coefficients related to the structure and material properties of the system and F_i is forcing term including the current density, volume of tetrahedral mesh and residual magnetic flux density.

$$K_{ij} = \begin{bmatrix} K_{xx} & K_{xy} & K_{xz} \\ K_{yx} & K_{yy} & K_{yz} \\ K_{zx} & K_{zy} & K_{zz} \end{bmatrix}, \quad \vec{A}_i = \begin{Bmatrix} A_{xi} \\ A_{yi} \\ A_{zi} \end{Bmatrix}, \quad \vec{F}_i = \begin{Bmatrix} F_{xi} \\ F_{yi} \\ F_{zi} \end{Bmatrix} \tag{8}$$

The individual elements of (8) can be expressed using tetrahedron volume V^e, permeability μ and coefficients b_i, c_i, d_j in (9). And details of coefficients include a coordinate of the vertex of a tetrahedron.

$$K_{xx} = \frac{1}{\mu}\frac{1}{36V^e}(c_ic_j + d_id_j),\ K_{xy} = -\frac{1}{\mu}\frac{1}{36V^e}c_ib_j,\ K_{xz} = -\frac{1}{\mu}\frac{1}{36V^e}d_ib_j$$

$$K_{yx} = -\frac{1}{\mu}\frac{1}{36V^e}b_ic_j,\ K_{yy} = \frac{1}{\mu}\frac{1}{36V^e}(b_ib_j + d_id_j),\ K_{yz} = -\frac{1}{\mu}\frac{1}{36V^e}d_ic_j$$

$$K_{zx} = -\frac{1}{\mu}\frac{1}{36V^e}b_id_j,\ K_{zy} = -\frac{1}{\mu}\frac{1}{36V^e}c_id_j,\ K_{zz} = \frac{1}{\mu}\frac{1}{36V^e}(b_ib_j - c_ic_j) \tag{9}$$

Forcing terms for each component are represented as follows.

$$F_{xi} = \frac{1}{\mu}\frac{1}{6}(B_{ry}d_i - B_{rz}c_i) + \frac{1}{4}V^eJ_{xi}$$

$$F_{yi} = \frac{1}{\mu}\frac{1}{6}(B_{rz}b_i - B_{rx}d_i) + \frac{1}{4}V^eJ_{yi} \tag{10}$$

$$F_{zi} = \frac{1}{\mu}\frac{1}{6}(B_{rx}c_i - B_{ry}b_i) + \frac{1}{4}V^eJ_{zi}$$

$$b_i = (-1)^i\{y_j(z_k - z_l) + y_k(z_l - z_j) + y_l(z_j - z_k)\}$$
$$c_i = (-1)^i\{z_j(x_k - x_l) + z_k(x_l - x_j) + z_l(x_j - x_k)\} \tag{11}$$
$$d_i = (-1)^i\{x_j(y_k - y_l) + x_k(y_l - y_j) + x_l(y_j - y_k)\}$$

where i, j, k, l = 1, 2, 3, 4 (cyclic permutation)

4. Analysis of Hall Effect Torque Sensor

4.1. Magnetic field profile of permanent magnet

When analyzing the torque sensor, it is important to know the characteristics of magnetization distribution for accurate analysis. A samarium cobalt magnet was used as an analysis model. The magnet is 20 [mm] in outside diameter, 15.5 [mm] in inside diameter, 4 [mm] in height. And the number of poles in the ring-type permanent magnet is 16 segments. The advantages of samarium cobalt are good quality related to temperature, and high remnant magnetic flux density and coercivity. On the other hand, the disadvantages are insufficient resource reserves, thus difficulty in securing it. Residual magnetic flux density of samarium cobalt is 1.149 [T] and coercivity 450 [kA/m]. The result can be illustrated as in Fig. 4 which shows the

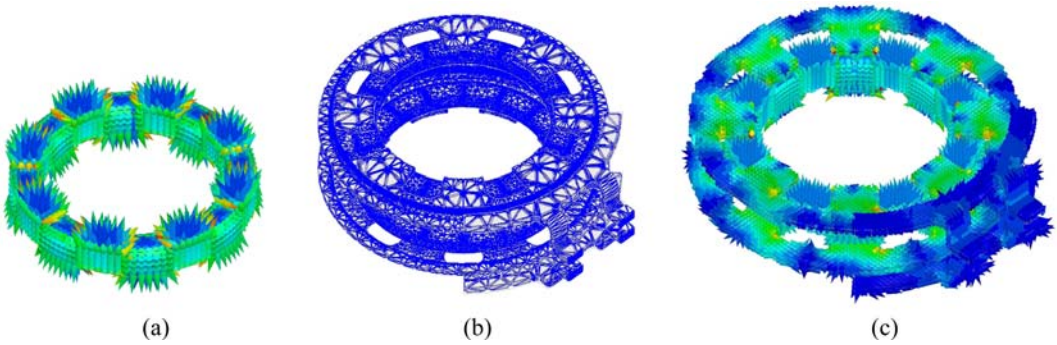

Fig. 4. (Color online) (a) Magnetic flux density distribution of permanent magnet, (b) Tetrahedral mesh and (c) magnetic flux density distribution of torque sensor in 3D finite element analysis.

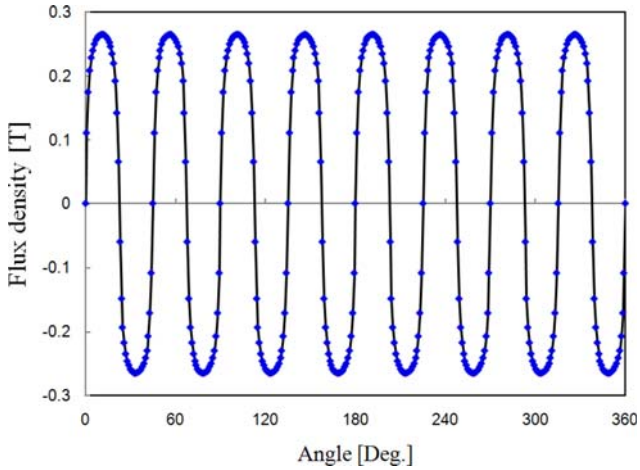

Fig. 5. (Color online) Calculated magnetic flux density profile along the surface of the permanent magnet.

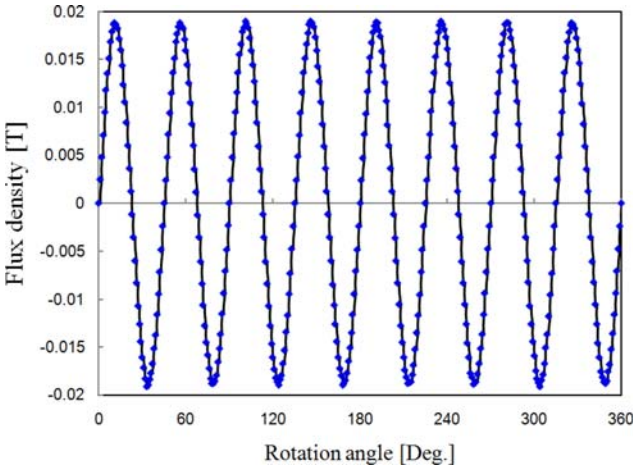

Fig. 6. (Color online) Magnetic flux density at the Hall sensor according to rotation angles.

finite element and magnetic flux density distribution of the torque sensor when the permanent magnet rotates 11° compared with reference position. When magnetic flux heads for z-axis, the magnetization distribution is bottom-up for N pole and top-down for S pole. When we measured the magnetic flux density 0.5 [mm] away from the surface of the permanent magnet, the result, as shown in Fig. 5, was obtained.

4.2. Magnetic field profile of torque sensor

Torque sensor used steering apparatus decide the magnitude and direction of supporting power sensing torque and rotating angle of steering wheel. So, the torque sensor using permanent magnet needs accurate analysis because the characteristic is sensitive to small movement and its structure is very complex. Also, torque sensor should generate changes of magnetic flux density to the rotating angle in specific operating ranges.

Magnetic field analysis of assembled Hall effect torque sensor was performed by using 3-dimensional finite element method. Fig. 6 shows the values of magnetic flux density at the Hall IC according to rotation angles of the permanent magnet of the torque sensor, ranging from 0° to 360°. It was found that the values of magnetic flux density are similar to sinusoidal curve. Fig. 7 shows the magnitude of magnetic flux density around the collector part using 3D arrow expression when the torque sensor rotates 11°.

Especially, the enlargement of the magnetic flux density profile when the torque sensor rotates from –22.5° to 22.5° is shown in Fig. 8(a) to know the linearity of flux density characteristic. Also, Fig. 8(b) shows more specific range with reference line. In range of operating angle about 4.5°, the characteristic of the torque sensor should satisfy linearity within this angle. Here the result of numerical analysis did satisfy the linearity in above ranges.

4.3. Shape design of stator teeth

Because torque sensors need accurate response characteristics, the following performance enhancements are

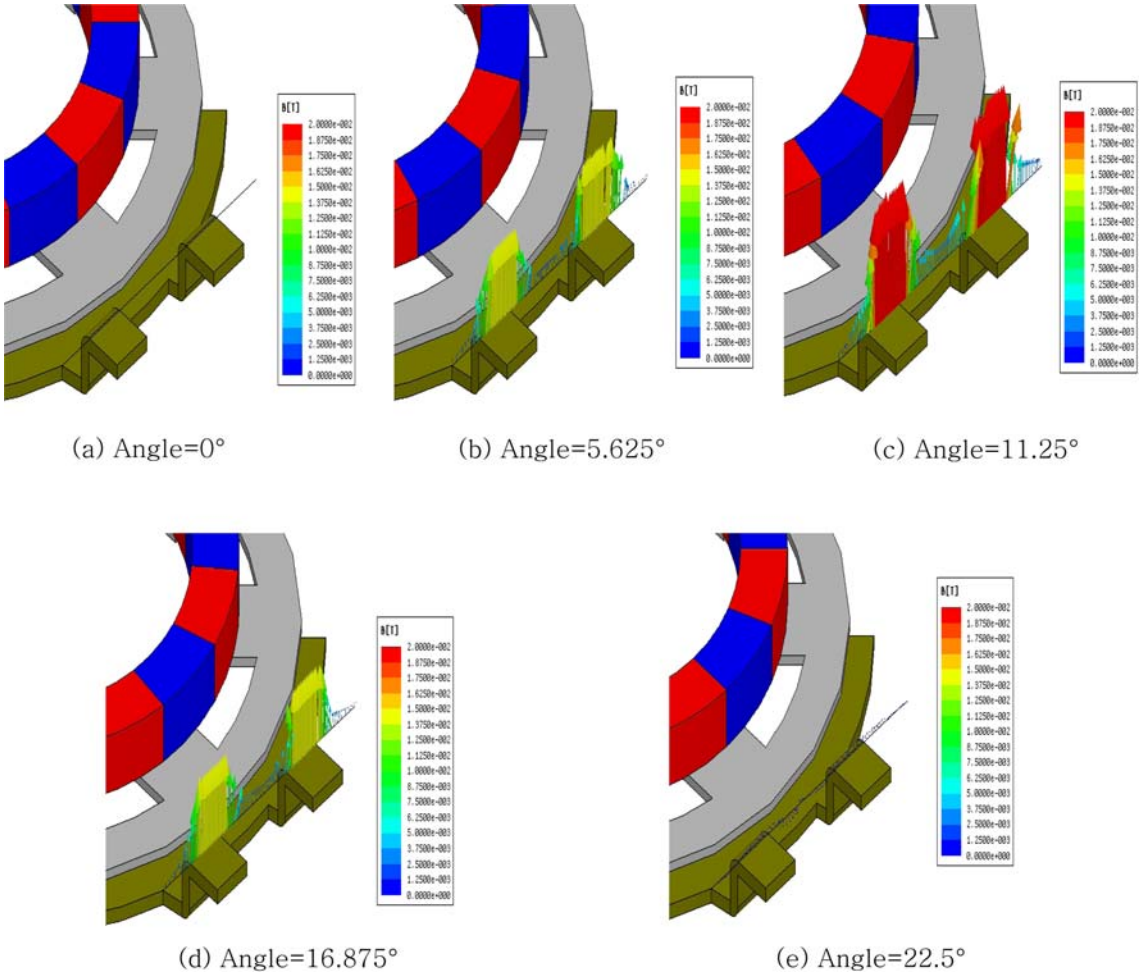

Fig. 7. (Color online) Magnetic flux density distributions around the collector according to the rotation angle. Magnitude of flux density is the maximum when the permanent magnet pole and stator teeth are aligned exactly.

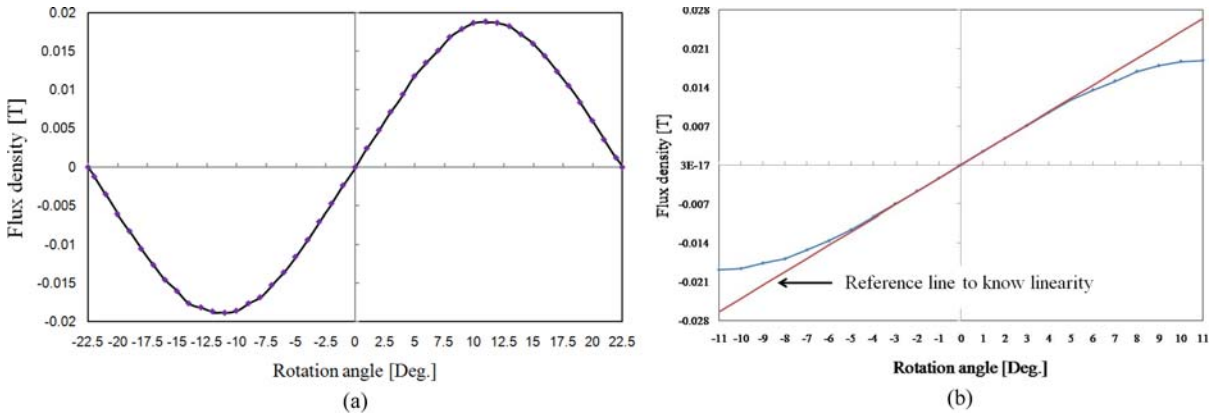

Fig. 8. (Color online) (a) Magnetic flux density of specific range (–22.5°~22.5°) and (b) compared view with linear reference.

required at the Hall sensor of collector. First, linearity of the flux characteristic should be large to get accurate information from the sensor. Secondly, linear range should be wide to assure the stability of the sensor. Finally, the magnetic flux density should be high to measure flux easily at the Hall IC.

The above enhancements, we proposed four kinds of stator teeth prototypes. The four prototypes named trian-

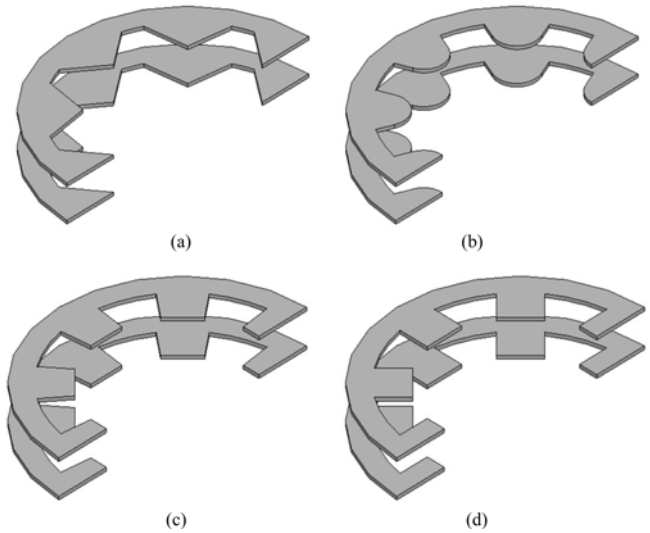

Fig. 9. Design shape of teeth for numerical analysis: (a) triangular type, (b) circular type, (c) trapezoidal type and (d) rectangular type.

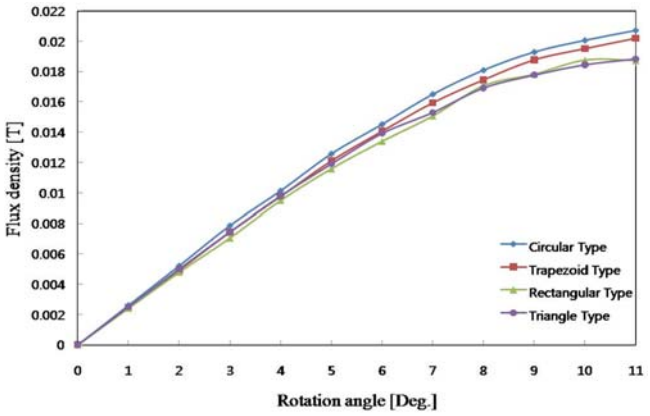

Fig. 10. (Color online) Magnetic flux density of various stator teeth shapes to compare its characteristic.

gular type, circular type, trapezoidal type and rectangular type are illustrated in Fig. 9. Magnetic field analysis for these types is performed to compare with each other.

Under the same condition for size, the researcher carried out the analysis of the 4 prototype. As a result, magnetic flux density varies according to the type of stator teeth as seen in Fig. 10. Among the 4 prototypes, the circular type achieved the highest values in linearity, linear range, and magnetic flux density.

5. Conclusion

This paper performed the characteristic analysis and shape design of stator teeth of Hall effect torque sensor used electric power steering system using 3D finite element method. Hall effect torque sensor using permanent magnet has complex structure and its characteristic is very sensitive to small mechanical movement. So, it is necessary for torque sensor to have linearity to operate wheels of the car accurately. After 3D finite element analysis of torque sensor, conclusions were obtained. First, the magnetic field of a torque sensor with complex 3D structure is accurately analyzed and characteristic curves of output flux at the collector are compared according to four shapes of stator teeth. Secondly, linear output flux profile of torque sensor with range of shift angles 4.5[°] ~ +4.5[°]. Finally, these results can predict the characteristics of torque sensor for various shape and permanent magnet array. Also, we will realize optimal design in a follow-up paper using the prototype that obtained the best result.

References

[1] C. H. Hu, Second International Symposium on IITA **3**, 436 (2008).
[2] A. W. Burton, IEEE Contr. Syst. Mag. **23**, 30 (2003).
[3] K. Miyashita, T. Takahashi, and S. Kawamta, IEEE Trans. Magn. **26**, 1560 (1990).
[4] D. Angleviel, D. Frachon, and G. Masson, SAE 2006-01-0939 (2006).
[5] W. H. Hayt, Engineering Electromagnetics, McGraw-Hill, New York (1989).
[6] S. J. Salon, Finite Element Analysis of Electrical Machines, Kluwer Academic, Norwell, MA (1995).
[7] M. A. Alhamadi, R. Wang, and N. A. Demerdash, IEEE Trans. Magn. **27**, 5016 (1991).
[8] P. Campbell, M. V. K. Chari, and J. D'Angelo, IEEE Trans. Magn. **17**, 2997 (1981).
[9] N. A. Demerdash, T. W. Nehl, F. A. Fouad, and O. A. Mohammed, IEEE Trans. Power Apparatus Sys. **100**, 4104 (1981).
[10] D. H. Im, Finite Element Method in Electrical Engineering, Dongmyeongsa, Seoul (1987).